J Incl Phenom Macrocycl Chem (2012) 74:231–238
DOI 10.1007/s10847-011-0104-6

ORIGINAL ARTICLE

Binding behavior of DEHP to albumin: spectroscopic investigation

Hua-xin Zhang · E Liu

Received: 8 November 2011 / Accepted: 15 December 2011 / Published online: 1 February 2012

Abstract Bis(2-ethylhexyl)phthalate (DEHP) is one of the biggest selling synthetic plasticizers which can migrate to environment and enter human body via air, water, medical apparatus, and food. In this paper, three-dimensional fluorescence (3D-FL) spectroscopy, UV–visible absorption spectroscopy and circular dichroism (CD) spectroscopy were employed to explore the binding of DEHP to bovine serum albumin (BSA) at the physiological conditions. The number of binding sites n and observed binding constant K_b was measured by fluorescence quenching method. It was found that the fluorescence quenching was static quenching mechanism and caused by the formation of DEHP–BSA complex at ground state. The enthalpy change (ΔH^{θ}), Gibbs free energy change (ΔG^{θ}) and entropy change (ΔS^{θ}) were calculated at four different temperatures. Site marker competitive displacement experiments were carried out to identify the binding location. The results demonstrated that DEHP bound primarily on Sudlow's site I in domain IIA of BSA molecule. The distance r (2.95 nm) between donor (BSA) and acceptor (DEHP) was obtained based on Förster's non-radiation fluorescence resonance energy transfer (FRET) theory. Furthermore, the CD spectral results indicated that the secondary structure of BSA changed in presence of high concentration of DEHP, which implied that high level of DEHP in plasma was potentially poisonous. The study is helpful to evaluating the health risk of DEHP and understanding its functional effects on protein during the blood transportation process.

H. Zhang (✉) · E Liu
College of Chemical and Pharmaceutical Engineering, Jingchu University of Technology, Jingmen 448000, Hubei, People's Republic of China
e-mail: h.x.zhang@yeah.net

Keywords DEHP · Bovine serum albumin · Three-dimensional fluorescence · Binding site · Energy transfer

Introduction

Bis(2-ethylhexyl)phthalate (CAS No.: 117-81-7; molecule structure: the inset of Fig. 3), also known as di(2-ethylhexyl)phthalate and commonly referred to as DEHP, is a liquid widely added in plastics (from 1 to 40% by weight) to make products more flexible. About 300 million pounds of DEHP are used each year in consumer products such as imitation leather, upholstery, toys, food packaging materials, tubing and containers for blood transfusions. Compared with DEHP levels commonly found in food and drinking water, DEHP that migrates from the plastics used in medical apparatus (such as storage bags and tubing) used for blood transfusions or kidney dialysis is much higher [1]. What is more serious is that the illegal use of DEHP as clouding agents in food and beverages, for the sake of low cost, has been exposed recently. Food safety issues that aroused by the use of DEHP as an additive has caused shock and panic among thousands of people and has attracted international attention. The risk of exposure to DEHP varies, being greatest by food and beverages, less by intravenous tubing and dialysis bags, still less by cosmetic chemical, and least by air and water [2]. The US EPA limits for DEHP in drinking water is 6 ppb. The US agency OSHA's limit for occupational exposure is 5 mg/m^3 of air. Excessive intake will be potential harmful [2, 3]. The carcinogenicity of DEHP and its adverse effects on reproductive health are well recognized by previous studies [4–6]. DEHP has been shown to cause liver tumors in both rats and mice receiving DEHP in their diet throughout their entire life span [7]. Studies regarding to the effects of

clinically relevant concentrations of DEHP on neonatal rat cardiomyocytes indicate that application of DEHP to a confluent, synchronously beating cardiac cell network, leads to a marked, concentration-dependent decrease in conduction velocity and asynchronous cell beating [8].

In spite of increasing number of animal studies conducted both in vitro and in vivo, have reported toxic effects of DEHP, it is difficult to estimate the kinds of health effects and exposure levels that may actually affect humans until these effects have been documented in humans. The human toxicity of DEHP continues to be a subject of intense debate between public health advocates, researchers and the industry [8] because there are essentially no studies on the health effects of DEHP in humans. Once DEHP gets into the gastrointestinal tract, it is quickly absorbed and following contact with blood, serum, or other albumin-containing fluids. So the investigations on the binding of DEHP to serum albumins are of great importance and necessity, which can provide information on the transportation, distribution, and toxicological behaviors of DEHP in vivo.

Serum albumins are the most abundant proteins in plasma and the main transport proteins, which are responsible for binding a diverse range of metabolites, drugs and chemical contaminants [9, 10]. In this work, bovine serum albumin (BSA) is selected as a protein model for its low cost and ready availability. The crystallographic analyses revealed that BSA is composed of three linearly arranged, structurally homologous domains (I–III) and each domain consists of two sub-domains (A, B) [11]. Two principal binding sites of ligand in serum albumin are located in hydrophobic cavities in sub-domains IIA and IIIA, also referred to as sites I and II, which can be marked by warfarin and ibuprofen, respectively [12]. Meanwhile, due to aromatic residues such as tryptophan, tyrosine and phenylalanine in its structure, BSA molecule gives intrinsic fluorescence, which allows this protein to be used in many biological applications by spectroscopic methods [13].

The aim of this paper is to investigate the molecular mechanism of the interaction between DEHP and BSA using spectroscopy methods and molecular probe techniques under physiological conditions in vitro. The interaction information with regard to quenching mechanism, binding constants, binding site, binding locality, thermodynamic parameters, binding power characteristics, energy transfer and conformational changes of BSA is to obtain.

Experimental

Materials

Bovine serum albumin was purchased from Sigma (USA, 99%). DEHP, Tris, HCl, NaCl were purchased from Shanghai Chemical Reagent Company (China). DEHP had a purity of no less than 99.5% and all other chemicals were of analytical grade. Stock solutions of BSA (10^{-5} mol L^{-1}), DEHP (2×10^{-3} mol L^{-1}), NaCl (0.5 mol L^{-1}) and Tris–HCl buffer (0.05 mol L^{-1} Tris, 0.15 mol L^{-1} HCl) of pH 7.40 ± 0.01 were prepared by directly dissolving the original reagents. Water used to prepare solutions was double-distilled.

Procedure and measurement

The buffer, NaCl, BSA and DEHP solutions were added with different ratios into several 10 mL colorimetric tubes, then diluted to 10 mL and stirred well. The solutions were let to stand for 5 min at room temperature, and then react for 30 min at specified temperatures.

All fluorescence spectra were recorded on a LS-55 Spectrofluorimeter (Perkin-Elmer, America) equipped with 1.0 cm quartz cells and a thermostat bath. The widths of the excitation slit and the emission slit were set to 15 and 2.5 nm with the scanning speed at 1,200 nm per minute. Appropriate blanks corresponding to the buffer were subtracted to correct the background. The UV spectra were recorded at room temperature on a UV-2450 spectrophotometer (Shimadzu, Japan) equipped with 1.0 cm quartz cells. The CD spectra were recorded in a J-810 spectropolarimeter (Jasco, Japan). The weight measurements were performed with an AY-120 electronic analytic weighing scale (Shimadzu, Japan). All pH measurements were made with a pHS-3 digital pH-meter (Shanghai, China).

Results and discussions

3D fluorescence spectra

Fluorescence occurs when an orbital electron of a molecule, atom or nanostructure relaxes to its ground state by emitting a photon of light after being excited to a higher quantum state by some type of energy. Fluorescence in the life sciences is used generally as a non-destructive way of tracking or analysis of biological molecules by means of the fluorescent emission at a specific frequency where there is no background from the excitation light [14–16]. Three-dimensional fluorescence (3D-FL) spectrum can provide abundant and all-side information on the structure of a phosphor as it is a stereopsis containing three coordinate axis including excitation wavelength, emission wavelength and fluorescence intensity. The 3D-FL spectra of BSA in and in no presence of DEHP were recorded and shown in Fig. 1. The information of fluorescence peaks is listed in Table 1. It is obvious that both position and stokes shift of fluorescence peaks of BSA altered when DEHP was added, which could be attributed to polarity changes of the region

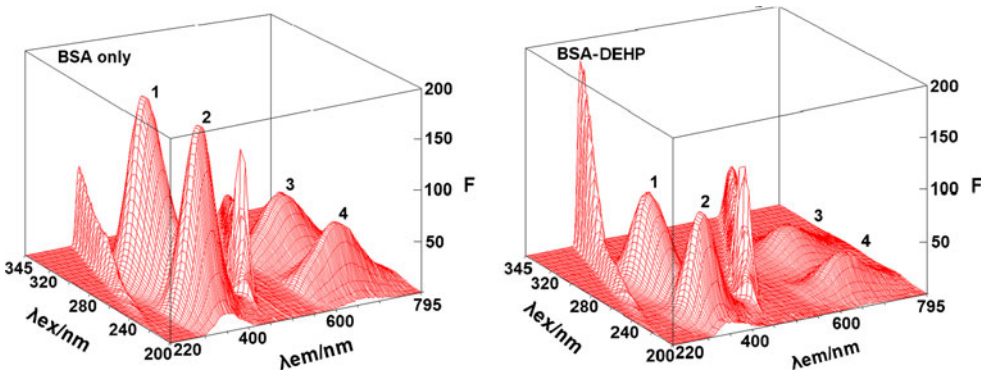

Fig. 1 Three-dimensional fluorescence spectra of BSA and DEHP–BSA complex (c_{BSA}: 2×10^{-6} mol L^{-1}, c_{DEHP}: 1.4×10^{-5} mol L^{-1})

surrounding the major chromophore in BSA. The intensity of all the four fluorescence peaks decreased with increasing amount of DEHP, which is commonly known as fluorescence quenching and may be caused by a variety of molecular interactions such as collisions, excited-state reactions, molecular rearrangements, energy transfer, ground-state complex formation, and so on [17].

Quenching mechanism analysis

Different fluorescence quenching processes can be divided into two broad categories, either dynamic quenching or static quenching [18]. In dynamic quenching, interaction between quencher and phosphor takes place during the lifetime of the excited state, in which no changes in absorption spectra will be observed. Moreover, dynamic quenching is caused by collision and higher temperature will result in larger diffusion coefficients, the dynamic quenching constants are expected to increase with increasing temperature [19]. In order to ascertain the quenching mechanism, the emission spectra of BSA and BSA–DEHP systems (the concentration of BSA was stabilized at 2×10^{-6} mol L^{-1}, and the concentration of DEHP varied from 0 to 1.4×10^{-5} mol L^{-1} at an increment of 2×10^{-6} mol L^{-1}) excited by 280 nm was picked out from their 3D-FL spectra and composed Fig. 2.

Supposing the quenching belong to dynamic quenching, the fluorescence data at different temperatures could be analyzed with the well-known Stern–Volmer equation [20]:

$$\frac{F_0}{F} = 1 + K_{SV}[Q] \quad (1)$$

where F_0 and F are the fluorescence intensities in absence and in presence of quencher, respectively, K_{SV} is the Stern–Volmer quenching constant, $[Q]$ is the concentration of the quencher. Hence, Eq 1 was applied to determine K_{SV} by linear regression of a plot of F_0/F against $[Q]$ (the inset of Fig. 2). The Stern–Volmer quenching constants K_{SV}, were calculated to be 7.769, 7.735, 7.709 and 7.681×10^4 L mol^{-1} at 298, 304, 310 and 316 K, respectively. This tendency is in conflict with the correlation of static quenching with temperature, which indicates that the more probable mechanism of DEHP–BSA interaction is static quenching rather than dynamic quenching. Moreover, the enhanced resonant scattering peaks in 3D-FL spectra (the left front of fluorescence peak 1 and peak 2 in Fig. 1) implies the presence of particle with different size, which is most likely to be the result of chemical binding. Absorption spectrum is an additional effective method to distinguish static and dynamic quenching [18]. The absorption spectra (Fig. 3) show that the absorbance of BSA–DEHP combination is weaker than that of the free BSA at equivalent concentration (2×10^{-6} mol L^{-1}), which can not make sense from the standpoint of dynamic quenching. Based on the discussion with respect to the temperature effects, scattering peaks and absorption spectra, as mentioned above, it is safely to draw the conclusion that the quenching of DEHP to BSA is static quenching mechanism.

Table 1 Characteristic parameters of three-dimensional fluorescence peaks

Systems and parameters		Peak 1	Peak 2	Peak 3	Peak 4
BSA	Peak position (λex/λem, nm/nm)	280.0/350.0	225.0/349.0	280.0/665.0	225.0/666.0
	Relative intensity	181.0	185.4	59.58	64.17
	Stokes shift $\Delta\lambda$/nm	70.0	124.0	385.0	441.0
BSA–DEHP	Peak position (λex/λem, nm/nm)	280.0/347.5	225.0/349.5	280.0/665.0	230.0/667.5
	Relative intensity	88.31	99.60	28.80	33.73
	Stokes shift $\Delta\lambda$/nm	67.5	124.5	385	437.5

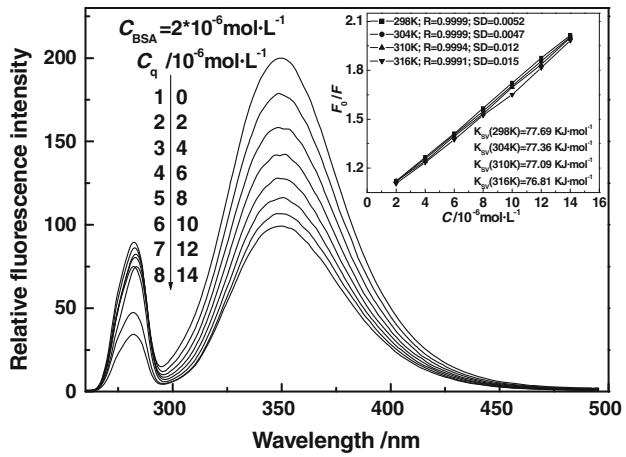

Fig. 2 Emission spectra of BSA in and in no presence of DEHP excited by 280 nm

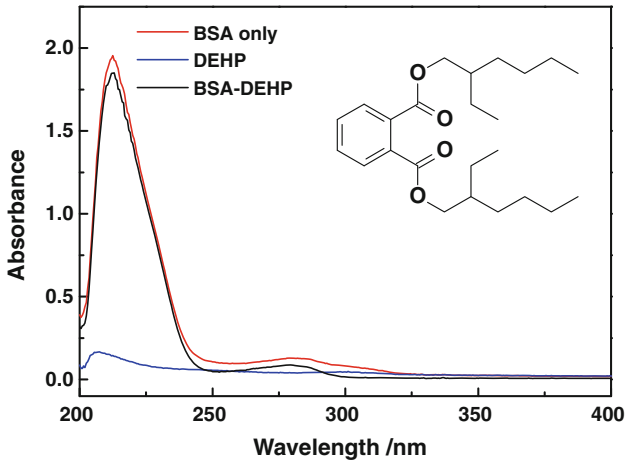

Fig. 3 Absorption spectra of DEHP, BSA and DEHP–BSA system

Binding equilibrium and thermodynamics

In the static quenching interaction, when small molecules bind independently to a set of equivalent sites on a macromolecule, the binding constant (K_b) and the number of binding sites (n) can be determined by the following equation [21]:

$$\log\left(\frac{F_0 - F}{F}\right) = \log K_b + n\log[Q] \tag{2}$$

The dependence of log $(F_0/F - 1)$ on the value of log $[Q]$ is linear with slope equal to the value of n and the value logK_b is fixed on the ordinate. The plots and the calculated results are shown in Fig. 4 and Table 2, respectively. Table 2 shows the number of binding site, n, are closed to 1, which indicates one high affinity binding site has formed between DEHP and BSA.

The enthalpy change and entropy change of DEHP–BSA interaction are important for confirming binding

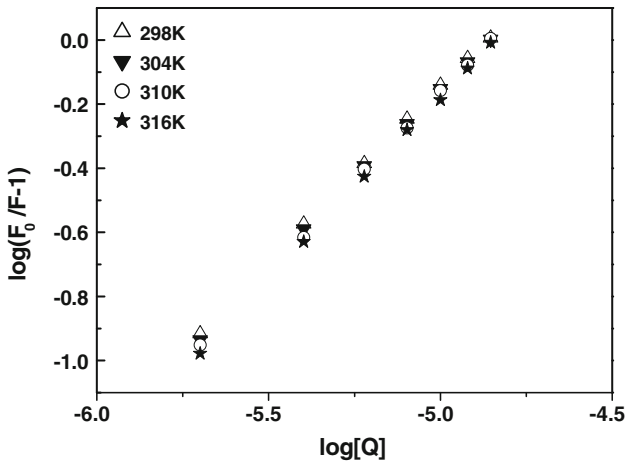

Fig. 4 Log $(F_0/F - 1)$–log$[Q]$ plots at four different temperatures

mechanism. Therefore, the temperature dependence of binding constant was studied using the Eqs. 3 and 4:

$$\ln K = \frac{-\Delta H^\theta}{RT} + \frac{\Delta S^\theta}{R} \tag{3}$$

$$\Delta G^\theta = \Delta H^\theta T \cdot \Delta S^\theta \tag{4}$$

where ΔH^θ, ΔG^θ and ΔS^θ are enthalpy change, Gibbs free energy change and entropy change, respectively. The plot of log$K$ versus $1/T$ (Fig. 5) enables the determination of ΔH^θ, ΔS^θ in isobaric processes while ΔG^θ can be calculated by Eq. 4. The results are listed in Table 2. The negative ΔG^θ and positive ΔS^θ indicate the interaction between DEHP and BSA is spontaneous and driven by entropy. Furthermore, according to the positive ΔH^θ, the reaction is an endothermic process, which can exactly give reasonable explanations for the increasing value of binding constant K_b and binding sites n (Table 2). Ross and Subramanian [22] thought that hydrophobic force might increase ΔH^θ and ΔS^θ of a system, hydrogen bond and van der Waals power decreased them, and electrostatic force usually made $\Delta H^\theta \approx 0$ and $\Delta S^\theta > 0$. Based on this rule, it can be speculated that hydrophobic forces play the major role during the interaction.

Site-selective binding geometry

There are two high affinity binding sites for drugs in BSA, site I locating in subdomain IIA and site II locating in subdomain IIIA, which can be marked by anticoagulant drug warfarin (inset of Fig. 6a) and antiinflammatory agent ibuprofen (inset of Fig. 6b), respectively [12]. In order to identify the binding site of DEHP on BSA, site marker competitive experiments were carried out using these two probes. In present experiment, DEHP was added to the solution of BSA that had been bound by site markers held in equivalent concentrations. Then the quenching effects

Table 2 Observed binding constants, binding sites and thermodynamic parameters

pH	T/(K)	K_b (L mol^{-1})	n	R	SD*	ΔH^θ (kJ mol^{-1})	ΔS^θ (J K^{-1})	ΔG^θ (kJ mol^{-1})
7.40	298	$10^{5.330}$	1.095	0.9998	0.0064	21.25	173.3	−30.40
	304	$10^{5.390}$	1.109	0.9999	0.0059			−31.44
	310	$10^{5.485}$	1.129	0.9999	0.0058			−32.48
	316	$10^{5.534}$	1.142	0.9999	0.0063			−33.52

* SD is the standard deviation for K_b

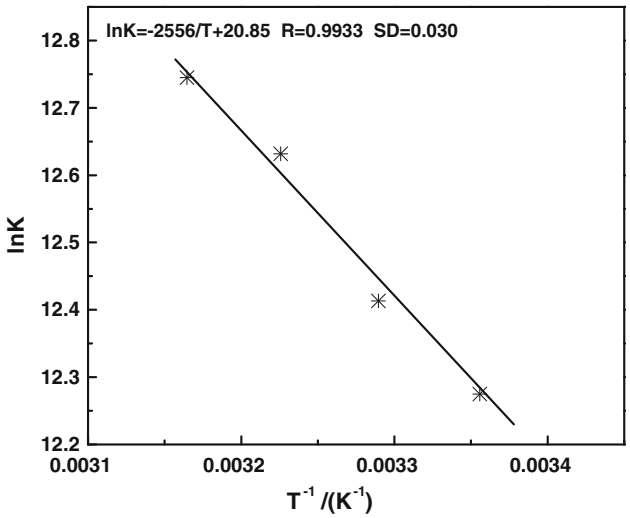

Fig. 5 Van't Hoff plot for the binding of DEHP with BSA

were measured and the results were shown in Fig. 6. It can be seen from Fig. 6a that warfarin which binds specifically to site I has more powerful ability to quench the luminescence of BSA than DEHP at equimolar concentration. When DEHP was added to BSA–warfarin system, an enhancement of the relative fluorescence intensity could be detected, which suggested that warfarin had been partially replaced by DEHP. In other word, DEHP had competed with warfarin for the site I in the subdomain IIA of BSA. On the other hand, in Fig. 6b, the binding of ibuprofen on site II in subdomain IIIA of BSA molecules seems to have no obvious influence on the binding of DEHP, which implies that DEHP bind on different site in protein from ibuprofen. To sum up the arguments above, DEHP bind with high affinity to site I in subdomain IIA of BSA. The conclusion is similar to the molecular docking results between DEHP and HSA reported by Xie et al. [23].

Energy transfer and binding distance

No distortion is found in the 3D-FL spectra (Fig. 1), which provides evidence for non-radiation energy transfer. According to Förster's non-radiation fluorescence resonance energy transfer (FRET) theory, the energy transfer efficiency is related not only to the distance between the acceptor and the donor but also to the critical energy transfer distance [24]:

$$E = \frac{R_0^6}{R_0^6 + r^6} \tag{5}$$

where E is the efficiency of transfer between the donor and the acceptor, R_0 is the critical distance when the efficiency of transfer is 50%, which can be calculated by the equation [25]:

$$R_0^6 = 8.8 \times 10^{-25} \left(K^2 \phi N^{-4} J\right) \tag{6}$$

where K^2 is the space factor of orientation; n is the refracted index of medium; ϕ is the fluorescence quantum yield of the donor; J is the effect of the spectral overlap between the emission spectrum of the donor and the

Fig. 6 Competitive binding of site markers and DEHP to BSA

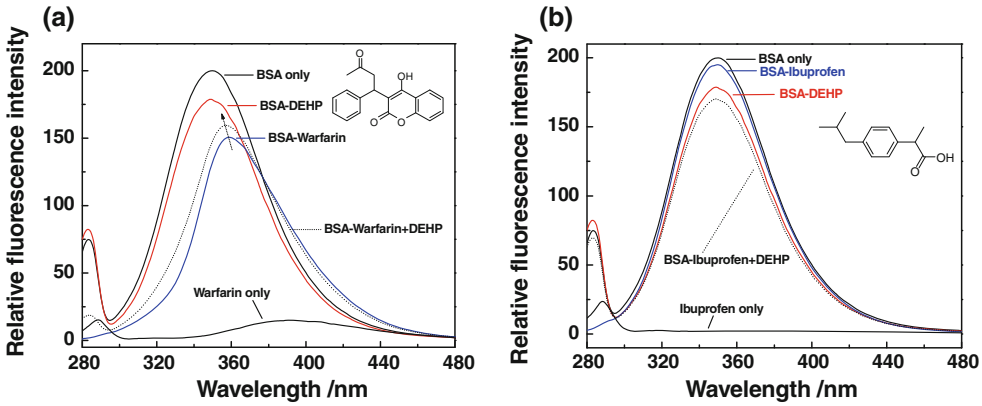

absorption spectrum of the acceptor, which could be calculated by the equation [24–26]:

$$J = \frac{\int_0^\infty F_D(\lambda)\varepsilon_A(\lambda_0)\lambda^4 d\lambda}{\int_0^\infty F_D(\lambda)d\lambda} \quad (7)$$

where $F_D(\lambda)$ is the corrected fluorescence intensity of the donor in the wavelength range λ_0 to λ, and $\varepsilon_A(\lambda_0)$ is the extinction coefficient of the acceptor at λ_0. The efficiency of transfer (E) could be obtained by the equation [25, 27]:

$$E = 1 - \frac{F}{F_0} \quad (8)$$

In the present case, $K^2 = 2/3$, $N = 1.36$ and $\phi = 0.15$ [28]. J could be obtained by integrating the UV absorption spectrum of DEHP and fluorescence emission spectrum of BSA (Fig. 7). According to the Eqs. 5–8, it is found that $J = 3.11 \times 10^{-13}\,\mathrm{cm^3\ L\ mol^{-1}}$; $E = 0.108$; $R_0 = 2.08$ nm; and the binding distance $r = 2.95$ nm. The distance r is shorter than 8 nm and in the range of 0.5–1.5R_0, which exactly falls in with Förster's premise and comes back to prove the probability of energy transfer from BSA to DEHP [29].

Conformation investigation

Synchronous fluorescence spectroscopy is a useful method to study the microenvironment of amino acid residues by measuring the emission wavelength shift because the shift in wavelength of emission maximum λ_{max} corresponds to the changes of polarity around the chromophore [30]. When the D-value ($\Delta\lambda$) between excitation and emission wavelength were stabilized at 60 and 15 nm, the synchronous fluorescence gives the characteristic information of tryptophan residues and tyrosine residues respectively. The synchronous fluorescence spectra of tryptophan (Fig. 8) and tyrosine (the inset of Fig. 8) were selected out from 3D-FL spectra. It shows the emission maximum λ_{max}

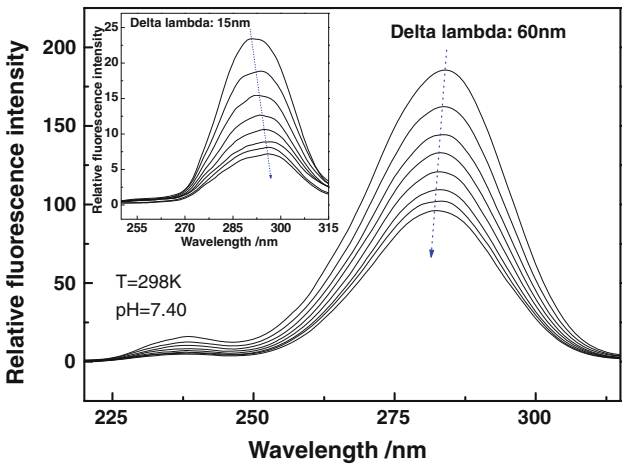

Fig. 8 Synchronous fluorescence spectra of tryptophan ($\Delta\lambda$ = 60 nm) and tyrosine ($\Delta\lambda$ = 15 nm)

of tryptophan residues shifts towards short wavelength (also called blue shift) while that of tyrosine residues shifts towards long wavelength (also called red shift), which means the polarity of tryptophan decreases after interactions with DEHP while tyrosine is just the reverse.

To further investigate the details of conformational changes of BSA, circular dichroism (CD) spectrum method was performed. CD spectrum is a sensitive technique to monitor the conformation of peptides and proteins because the structural characterization of proteins depends greatly on the remarkable sensitivity of CD in far-UV region [31]. CD spectrum of BSA exhibits two negative bands at 208 and 222 nm which reflect the characteristic of α-helix in the advanced structure of protein as these two negative peaks are both contributed to $n \rightarrow \pi^*$ transfer for the peptide bond of α-helical. CD results can be expressed in terms of mean residue ellipticity (MRE) in deg $\mathrm{cm^2}$ d $\mathrm{mol^{-1}}$ according to the following equation [32]:

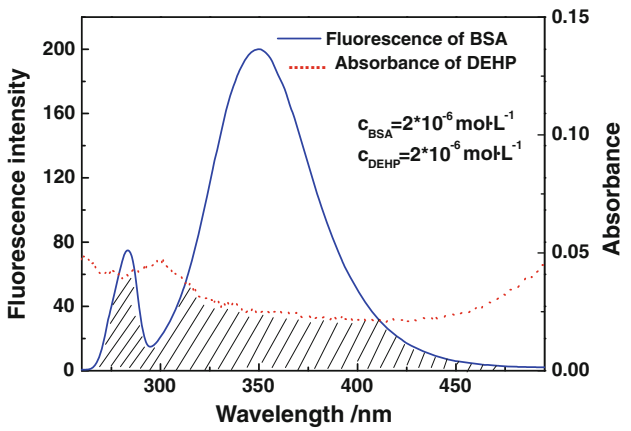

Fig. 7 Absorption spectrum of DEHP and fluorescence emission spectrum of BSA

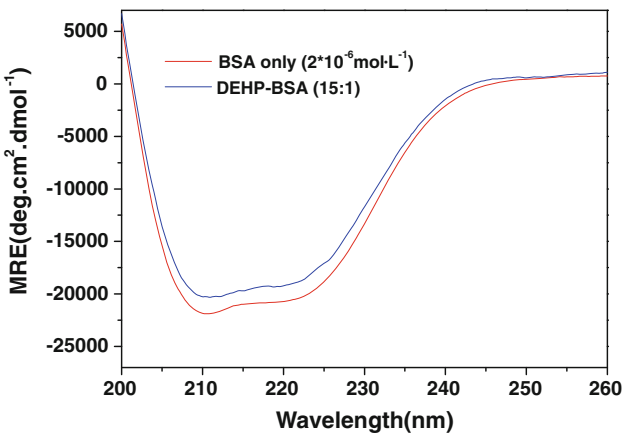

Fig. 9 The CD spectrum of BSA and DEHP–BSA system

Table 3 Fractions of different secondary structures

Molar ratio [DEHP]:[HSA]	H(r) (%)	H(d) (%)	S(r) (%)	S(d) (%)	Trn (%)	Unrd (%)
0:1	40.2	19.6	2.9	3.0	12.9	20.8
15:1	36.9	19.6	3.5	3.7	15.1	21.9

H(r) regular α-helix, *H(d)* distorted α-helix, *S(r)* regular *β*-strand, *S(d)* distorted *β*-strand, *Trn* turns, *Unrd* unordered structure

$$MRE = \frac{Observed\ CD(m^{\circ})}{C_{\mathrm{p}}nl \times 10} \tag{9}$$

where C_{p} is the molar concentration of the protein, n the number of amino acid residues and l is the path length (0.1 cm). The α-helical contents of free and combined BSA were calculated from MRE values at 208 nm using the equation [33]:

$$\alpha\text{-}helix(\%) = \frac{-MRE_{208} - 4{,}000}{33{,}000 - 4{,}000} \tag{10}$$

where MRE_{208} is the observed MRE value at 208 nm, 4,000 is the MRE of the *β*-form and random coil conformation cross at 208 nm and 33,000 is the MRE value of a pure α-helix at 208 nm. Using Eq. 10, the α-helicity in the secondary structure of BSA was determined and results were pasted on Fig. 9 and the estimates for the secondary structural elements analyzed using SELCON3 software are listed in Table 3. In Table 3, a reduction of the α-helix from 59.8% (free BSA) to 56.5% was observed (at molar ratio of 15:1). Then combining the discussion of binding forces and synchronous fluorescence spectra above, hydrophobic forces leaded to the loosening and unfolding of the protein skeleton, in which process the microenvironment of the tryptophan (Trp-212) became more hydrophobic but tyrosine (Tyr-263) was more hydrophilic. It once again, indicated that DEHP was buried in the hydrophobic cave around site I in subdomain IIA of BSA. The entering compelled Tyr-263 to move out from original cave and more expose to solvent, which indicated that the combination of DEHP to BSA could destroy the secondary structure of BSA and following affect its physiological function. Nevertheless, this effect was not obvious until the concentration of DEHP reached 3×10^{-5} mol L^{-1}.

Conclusions

In present paper, three-dimensional fluorescence (3D-FL) spectroscopy, UV–vis spectroscopy and circular dichroism (CD) spectroscopy were used to investigate the interaction of DEHP with BSA in vitro. Under physiological conditions, DEHP and BSA formed new complex by hydrophobic interactions at ground state, accompanied with static fluorescence quenching and non-radiation energy transfer happening within a single molecule. The binding constants K_{b} are of the order 10^5 L mol^{-1} and one high affinity binding site has formed between DEHP and BSA. Site-selective competitive binding investigation indicated that the binding site located in Sudlow's site I in sub-domains IIA of BSA and the distance r between DEHP and Trp-212 in BSA was calculated to be 2.95 nm according to Förster's non-radiation fluorescence resonance energy transfer (FRET) theory. The interaction was a spontaneous as well as an entropy-driven process based on the thermodynamic parameters obtained under atmospheric pressure conditions. The large K_{b} ($10^{5.485}$ L mol^{-1}) at 310 K indicated that the degree of reversibility was not pronounced around body temperature, which gave a hint that DEHP could be transported and stored in blood. A reduction of the α-helix from 59.8% (free BSA) to 56.5%, along with changes of other elaborate second-order structures contents was detected when the concentration of DEHP reached 3×10^{-5} mol L^{-1}. These surveys provided comprehensive basic data for understanding the binding mechanism of DEHP with albumin and were expected to give useful clues to the clarification of the ways of albumin acting as a detoxifier for DEHP.

Acknowledgments The authors gratefully acknowledge the fund support of Science and Technology Research Program of the Education Department, Hubei, China (Grant No. B20104301) and Scientific Research Project of Jingchu University of Technology (Grant No. ZR200905; ZR201014).

References

1. Mettang, T., Pauli-Magnus, C., Alscher, D., Kirchgessner, J., Wodarz, R., Rettenmeier, A., Kuhlmann, U.: Influence of plasticizer-free CAPD bags and tubings on serum, urine, and dialysate levels of phthalic acid esters in CAPD patients. Perit. Dial. Int. **20**, 80–84 (2000)
2. Barr, D.B., Silva, M.J., Kato, K., Reidy, J.A., Malek, N.A., Hurtz, D., Sadowski, M., Needham, L.L., Calafat, A.M.: Assessing human exposure to phthalates using monoesters and their oxidized metabolites as biomarkers. Environ. Health Perspect. **111**, 1148–1151 (2003)
3. Albro, P., Corbett, J., Schroeder, J., Jordan, S., Matthews, H.: Pharmacokinetics, interactions with macromolecules and species differences in metabolism of DEHP. Environ. Health Perspect. **45**, 19–25 (1982)
4. Doull, J., Cattley, R., Elcombe, C., Lake, B.G., Swenberg, J., Wilkinson, C., Williams, G., van Gemert, M.: A cancer risk assessment of di(2-ethylhexyl)phthalate: application of the New U.S. EPA risk assessment guidelines. Regul. Toxicol. Pharm. **29**, 327–357 (1999)

5. Gray, T., Beamand, J.: Effect of some phthalate esters and other testicular toxins on primary cultures of testicular cells. Food Chem. Toxicol. **22**, 123–131 (1984)
6. Noriega, N.C., Howdeshell, K.L., Furr, J., Lambright, C.R., Wilson, V.S., Gray, L.E.: Pubertal administration of DEHP delays puberty, suppresses testosterone production, and inhibits reproductive tract development in male Sprague–Dawley and long-evans rats. Toxicol. Sci. **111**, 163–178 (2009)
7. Ganning, A.E., Olsson, M.J., Brunk, U., Dallner, G.: Effects of prolonged treatment with phthalate ester on rat liver. Pharmacol. Toxicol. **67**, 392–401 (1990)
8. Gillum, N., Karabekian, Z., Swift, L.M., Brown, R.P., Kay, M.W., Sarvazyan, N.: Clinically relevant concentrations of di (2-ethylhexyl) phthalate (DEHP) uncouple cardiac syncytium. Toxicol. Appl. Pharm. **236**, 25–38 (2009)
9. Silva, E., Rousseau, C., Zanella-Cléon, I., Becchi, M., Coleman, A.: Mass spectrometric determination of association constants of bovine serum albumin (BSA) with para-sulphonato-calix[n] arene derivatives. J. Incl. Phenom. Macro. **54**, 53–59 (2006)
10. Giardiello, M., Botta, M., Lowe, M.: Synthesis of lanthanide(III) complexes appended with a diphenylphosphinamide and their interaction with human serum albumin. J. Incl. Phenom. Macro. (2011). doi: 10.1007/s10847-011-0009-4
11. Carter, D.C., Ho, J.X.: The structure of serum albumin. Adv. Protein Chem. **45**, 153–203 (1994)
12. Roy, A.S., Tripathy, D.R., Chatterjee, A., Dasgupta, S.: A spectroscopic study of the interaction of the antioxidant naringin with bovine serum albumin. J. Biophys. Chem. **1**, 141–152 (2010)
13. Sochacka, J., Sulkowska, A., Kowalska, A.: The binding of the sulfur and oxygen purine derivatives with bovine serum albumin. Acta Pol. Pharm. **65**, 169–171 (2008)
14. Klajnert, B., Bryszewska, M.: Fluorescence studies on PAMAM dendrimers interactions with bovine serum albumin. Bioelectrochemistry **55**, 33–35 (2002)
15. Ghosh, S.K., Hossain, S.U., Bhattacharya, S., Bhattacharya, S.C.: 2-(2-Selenocyanic acid ethyl ester)-1H-benz[de] isoquinoline-1, 3-(2H)-dione, synthesis photophysics and interaction with bovine serum albumin: a spectroscopic approach. J. Photochem. Photobiol. B **81**, 121–128 (2005)
16. Shcharbin, D., Klajnert, B., Mazhul, V., Bryszewska, M.: Dendrimer interaction with hydrophobic fluorescent probes and human serum albumin. J. Fluoresc. **15**, 21–28 (2005)
17. Boghaei, D.M., Farvid, S.S., Gharagozlou, M.: Interaction of copper(II) complex of compartmental Schiff base ligand N, N'-bis(3-hydroxysalicylidene)ethylenediamine with bovine serum albumin. Spectrochim. Acta A **66**, 650–655 (2007)
18. Hu, Y.J., Ou-Yang, Y., Dai, C.M., Liu, Y., Xiao, X.H.: Site-selective binding of human serum albumin by Palmatine: spectroscopic approach. Biomacromolecules **11**, 106–112 (2010)
19. Gharagozlou, M., Boghaei, D.M.: Interaction of water-soluble amino acid Schiff base complexes with bovine serum albumin: fluorescence and circular dichroism studies. Spectrochim. Acta A **71**, 1617–1622 (2008)
20. Sułkowska, A., Równicka, J., Bojko, B., Sułkowski, W.: Interaction of anticancer drugs with human and bovine. J. Mol. Struct. **651–653**, 133–140 (2003)
21. Chi, Z.X., Liu, R.T.: Phenotypic characterization of the binding of tetracycline to human serum albumin. Biomacromolecules **12**, 203–209 (2011)
22. Ross, P.D., Subramanian, S.: Thermodynamics of protein association reactions: forces contributing to stability. Biochemistry **20**, 3096–3102 (1981)
23. Xie, X., Wang, Z., Zhou, X., Wang, X., Chen, X.: Study on the interaction of phthalate esters to human serum albumin by steady-state and time-resolved fluorescence and circular dichroism spectroscopy. J. Hazard. Mater. (2011). doi:10.1016/j.jhazmat.2011.06.038
24. Ashoka, S., Seetharamappa, J., Kandagal, P.B., Shaikh, S.M.T.: Investigation of the interaction between trazodone hydrochloride and bovine serum albumin. J. Lumin. **121**, 179–186 (2006)
25. Zhang, H.X., Gao, S., Xiong, Z.Y., Liu, S.P.: Fluorometric probing on the binding of hematoxylin to serum albumin. Mol. Biol. Rep. **36**, 2299–2306 (2009)
26. Kamat, B.P.: Study of the interaction between fluoroquinolones and bovine serum albumin. J. Pharm. Biomed. **39**, 1046–1050 (2005)
27. Shaikh, S.M.T., Seetharamappa, J., Ashoka, S., Kandagal, P.B.: A study of the interaction between bromopyrogallol red and bovine serum albumin by spectroscopic methods. Dyes Pigments **73**, 211–216 (2007)
28. Hu, Y.J., Wang, Y., Ou-Yang, Y., Zhou, J., Liu, Y.: Characterize the interaction between naringenin and bovine serum albumin using spectroscopic approach. J. Lumin. **130**, 1394–1399 (2010)
29. Förster, T.: Intermolecular energy migration and fluorescence. Ann. Phys. **437**, 55–75 (1948)
30. Zhang, H.X., Mei, P., Yang, X.X.: Optical, structural and thermodynamic properties of the interaction between tradimefon and serum albumin. Spectrochim. Acta A **72**, 621–626 (2009)
31. Bulheller, B.M., Rodger, A., Hirst, J.D.: Circular and linear dichroism of proteins. Phys. Chem. Chem. Phys. **9**, 2020–2035 (2007)
32. Rogers, D.M., Hirst, J.D.: First-principles calculations of protein circular dichroism in the near ultraviolet. Biochemistry **43**, 11092–11102 (2004)
33. Whitmore, L., Wallace, B.A.: Protein secondary structure analyses from circular dichroism spectroscopy methods and reference databases. Biopolymers **89**, 392–400 (2007)